Supplementary Information for

Mechanically and electrically biocompatible hydrogel ionotronic fibers for fabricating structurally stable implants and enabling noncontact physioelectrical modulation

Zhihao Chen[a], Taiwei Zhang[b], ChunTeh Chen[c], Shuo Yang[a], Zhuochen Lv[a], Leitao Cao[a], Jing Ren[a], Zhengzhong Shao[d], Li-bo Jiang[b], and Shengjie Ling[*a]

[a]School of Physical Science and Technology, ShanghaiTech University, 393 Middle Huaxia Road, Shanghai, 201210 China

[b]Department of Orthopedic Surgery, Zhongshan Hospital, Fudan University, No. 180, Fenglin Road, Shanghai 200032, China

[c]Department of Materials Science and Engineering, University of California, Berkeley 94720 CA, USA

[d]State Key Laboratory of Molecular Engineering of Polymers, Department of Macromolecular Science, Laboratory of Advanced Materials, Fudan University, Shanghai, 200433, China

* Correspondence and requests for materials should be addressed to:
lingshj@shanghaitech.edu.cn (S. Ling)

This file includes:

Supplementary Note 1. A five-parameter linear solid model to model the MT-induced structural and mechanical evolution.

MT-AHIFs possess acquired highly oriented molecular cross-linking network (MCN). Grid model (**Figure S5**) can be involved to model the structural evolution induced by MT process. At the very beginning of MT process, nearly all the grids were randomly oriented, and then MCN starts to acquire the tendency to align along the axial direction of external load. In the perspective of one local β-grid, if four adjacent α-grids form axial orientation, the local β-grid which works as the joint at the chain center should then tend to join the overall alignment and then those five grids form a oriented α-β unit. The MT-AHIFs is then regarded as a collection of oriented α-β units (**Figure S5**). In such a MT process, exchange of internal ions, entanglement of chains and possible migration of nanocrystals are allowed, which might lead to the fluctuation of the strength in each tensile cycle, yet the increasing trend of modulus is not influenced.

The orientation procedure of α-grids, in this case, can be related to the yielding and be presented by one relaxation spring (E_1); On the other hand, the orientation procedure of β-grids contributes to non-linear viscoelastic mechanical behaviors like hardening and can be presented by one reversed relaxation spring (E_2). Of note, $E_1E_2 \leq 0$. E_t is introduced to describe the orientation-induced termination modulus of each cycle. For yielding and hardening, two dashpots are involved to describe dissipations of energy for varied mechanical behaviors, respectively. The constitutive equation of such a grid model (5-parameter viscoelastic model) is expressed as[1,2]:

$$\sigma(t) = \dot{\varepsilon}E_t t + \sum_{i=1}^{n} \dot{\varepsilon}E_i\tau_i\left(1 - e^{\left(-\frac{t}{\tau_i}\right)}\right)$$

Notably, n should equal to 2 for 5-paramter model, and all the fitting parameters are listed in **Table S2**. All the parameters are extracted through the stress-strain curve of each loop[1].

Supplementary Note 2. Alginate is a copolymer of guluronic (G) and mannuronic (M) units. The units are arranged in repeating blocks of GG, MM, or GM. The CGMD model of AHIF consists of three types of beads: GG-block beads (type-1), MM- and GM-block beads (type-2), and calcium ion beads (type-3). Each GG-block bead represents two GG-blocks (four G sequences). Similarly, each MM- and GM-block bead represents two MM- or GM-blocks. The calcium ion bead represents two calcium ions. The weight of alginate chains was measured as 80 to 350 kDa[3,4], corresponding to 450 to 2,000 sequences. To match the conditions of experimental observations, each alginate chain consists of 200 alginate beads (800 sequences). The ratio of GG-blocks was reported as 0.16[5]. Thus, among the 200 alginate beads, 32 of them are randomly selected to be GG-block beads and the others are MM- or GM-block beads. In alginate hydrogel, GG-blocks can form crosslinks with calcium ions but MM- and GM-blocks cannot form such crosslinks. The difference between the contributions of MM-blocks

and GM-blocks is negligible to the mechanical properties of alginate hydrogel. To reduce the complexity of the CGMD model, MM- and GM-blocks are represented by the same alginate beads (type-2). The model consists of 512 alginate chains with a total of 102,400 alginate beads and 8,192 calcium ion beads. Alginate beads are connected by linear springs with the bond energy described by the harmonic potential as:

$$E_{bond} = \frac{1}{2}K_{bond}(r - r_0)^2$$

where K_{bond} is the stiffness of the bond, r is the distance between two neighboring alginate beads, and r_0 is the equilibrium distance. The bending stiffness of alginate chains is provided by angular springs with the bending energy described by the harmonic potential as:

$$E_{angle} = \frac{1}{2}K_{angle}(\theta - \theta_0)^2$$

where K_{angle} is the bending stiffness, θ is the angle defined by three neighboring alginate beads, θ_0 is the equilibrium angle. The non-bonded interactions between beads are described by the Lennard-Jones (LJ) potential with a distance shifted by delta:

$$E_{LJ} = 4\epsilon\left[\left(\frac{\sigma}{r - \Delta}\right)^{12} - \left(\frac{\sigma}{r - \Delta}\right)^{6}\right]$$

where ϵ is the depth of the potential well, σ is the zero-crossing distance, and Δ is the shifted distance characterizing the size of beads. The parameters adopted in this work are summarized in **Table S3**. The timestep is set to 0.1 ps and periodic boundary conditions are imposed. Three steps of simulations are implemented to generate an equilibrium structure of the model. In the first step, the model is equilibrated with an isothermal–isobaric (NPT) ensemble at a constant temperature of 600 K and pressure of 10 KPa for 1 μs. The non-bonded interactions between the beads are set to 1% of the original values. The high temperature and low non-bonded interactions allow alginate chains to form a randomly-oriented molecular network. The initial pressure prevents the model to become unstable during the high-temperature simulation. In the second step, the interactions between the beads are set to the original values and the model is equilibrated with the same NPT ensemble for another 1 μs. In the third step, the model is equilibrated with an NPT ensemble at a constant temperature of 300 K and zero pressure for another 1 μs. After the three steps of simulations, the equilibrium structure is adopted for mechanical training. In the loading step, the model is equilibrated with an NPT ensemble at a constant temperature of 300 K and tensile stress increasing from zero to 100 KPa for 100 ns. In the unloading step, the model is equilibrated with an NPT ensemble at a constant temperature of 300 K and tensile stress decreasing from 100 KPa to zero for 100 ns. These two steps of loading and unloading simulations are repeated 300 times. The simulations were performed using Large-scale Atomic/Molecular Massively Parallel Simulator (LAMMPS)[6].

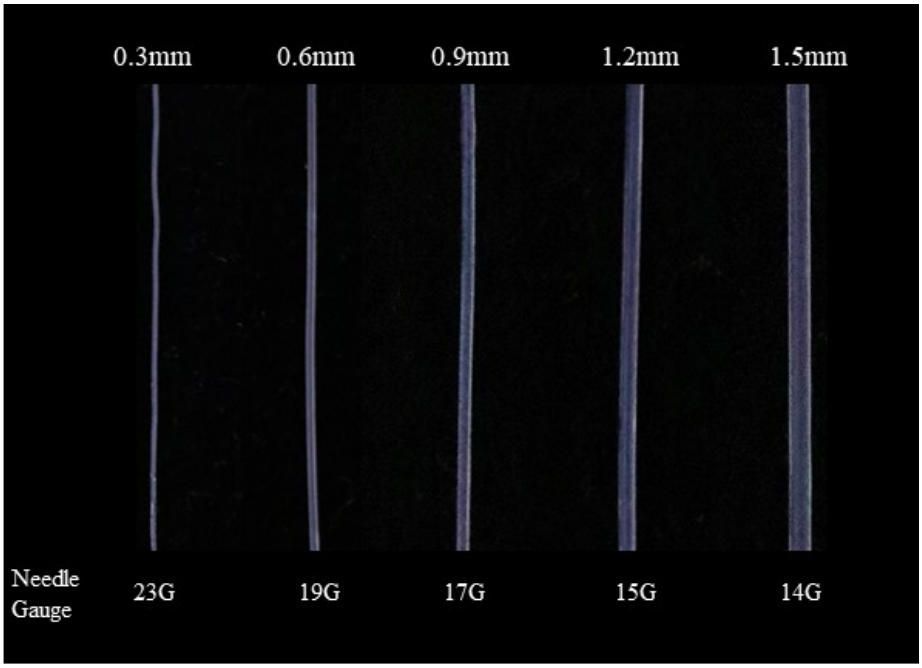

Supplementary Figure 1: AHIFs of the different diameters.

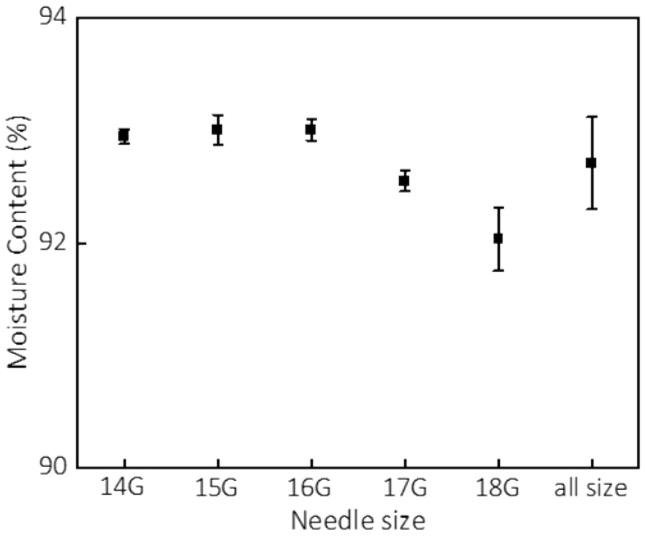

Supplementary Figure 2: Water content of the AHIFs of different diameters .

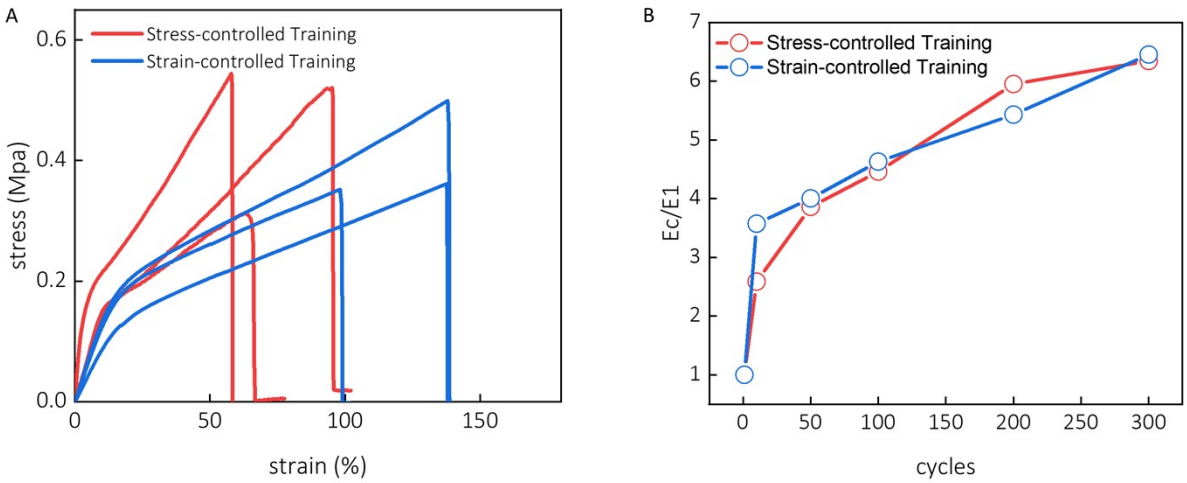

Supplementary Figure 3: Orientation and mechanical properties of AHIFs under constant stress mode and constant strain mode.

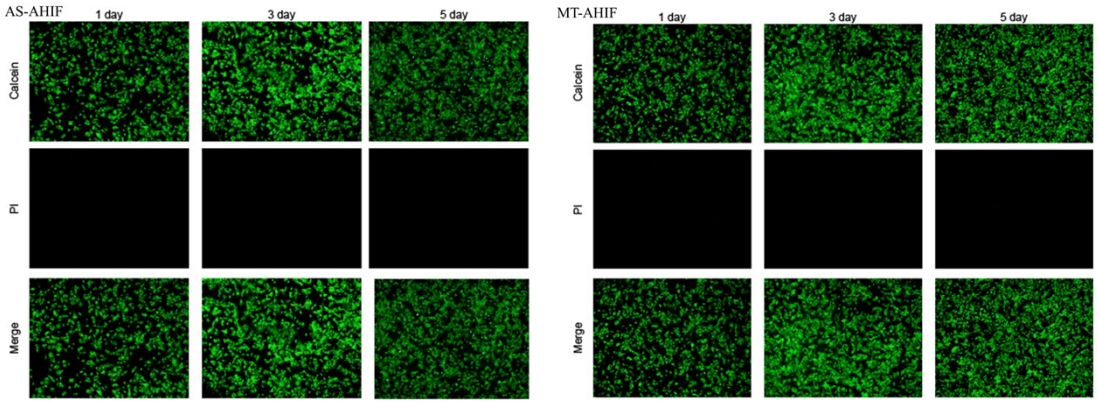

Supplementary Figure 4: Live/dead cell staining of BMSCs seeded on different materials for 1,3,5 days;

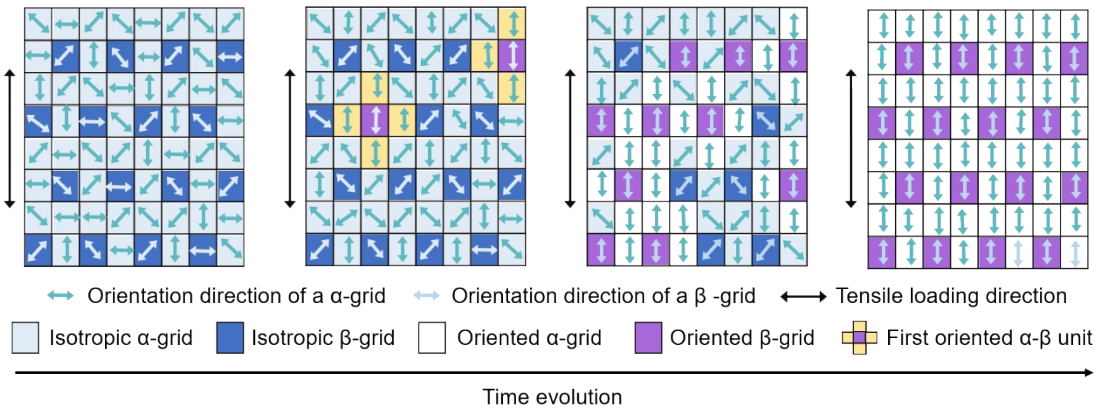

Supplementary Figure 5: Grid model, which is associated with five-parameter linear solid model, shows the structure evolution during mechanical training process.

Table S1. The mechanical properties of AHIFS

Name	Strength (MPa)	Young's Modulus (MPa)	Failure Strain (%)
AS-AHIF	0.47±0.12	0.1±0.001	185.4±38.9
10cycles-AHIF	0.59±0.10	0.7±0.4	155.1±35.2
20cycles-AHIF	0.54±0.14	1.0±0.5	147.0±29.6
50cycles-AHIF	0.49±0.14	1.2±0.6	117.9±11.3
100cycles-AHIF	0.58±0.08	1.6±0.9	143.9±45.1
200cycles-AHIF	0.54±0.09	1.9±1.0	77.0±22.5
MT-AHIF	0.6±0.1	2.6±1.1	227.7±36.0

* The number-cycles in the name represents the mechanical training cycles.

Table S2. Fitting parameters for five-parameter linear solid model.

	E_2 (KPa)		E_t (KPa)		τ (s)	
Loop	Load	Unload	Load	Unload	Load	Unload
5	-0.90	-2.51	1.24	2.86	0.65	0.53
10	-1.15	-2.57	1.36	2.79	0.53	0.49
20	-1.04	-2.35	1.43	2.65	0.29	0.37
50	-1.39	-2.60	1.74	2.87	0.24	0.31
100	-1.38	-2.87	1.96	3.17	0.24	0.30
200	-1.66	-2.98	2.33	3.32	0.18	0.30

* E_1 is regarded to be 0 and τ_1 equals τ_2 in this case since all the stress-strain curves

are J-shape or near J-shape. For S-shape curves, E_1 is larger than zero and τ_1 varies from τ_2.

Table S3. Summary of parameters for the CGMD model.

Parameter	**Value**
Bond stiffness, K_{bond} (kg/s^2)	0.2
Equilibrium distance, r_0 (nm)	2
Bending stiffness, K_{angle} $(kg \cdot nm^2/s^2/rad^2)$	0.2
Equilibrium angle, θ_0 (degree)	180
Pair potential, LJ distance parameter, $\sigma_{1,1}$, $\sigma_{2,2}$, $\sigma_{3,3}$, $\sigma_{1,2}$, $\sigma_{2,3}$ (nm)	1.0
Pair potential, LJ distance parameter, $\sigma_{1,3}$ (nm)	0.5
Pair potential, LJ shifted distance parameter, $\Delta_{1,1}$, $\Delta_{2,2}$, $\Delta_{3,3}$, $\Delta_{1,2}$, $\Delta_{2,3}$ (nm)	0.5
Pair potential, LJ shifted distance parameter, $\Delta_{1,3}$ (nm)	0.25
Pair potential, LJ energy parameter, $\epsilon_{1,1}$, $\epsilon_{2,2}$, $\epsilon_{3,3}$, $\epsilon_{1,2}$, $\epsilon_{2,3}$ $(kg \cdot nm^2/s^2)$	0.0007
Pair potential, LJ energy parameter, $\epsilon_{1,3}$ $(kg \cdot nm^2/s^2)$	0.07
Mass of mesoscale bead, m_1, m_2 (attogram)	0.06
Mass of mesoscale bead, m_3 (attogram)	0.006

References

1. Lv, Z., et al. Mechanism of mechanical training-induced self-reinforced viscoelastic behavior of highly hydrated silk materials. *Biomacromolecules* **22**, 2189-2196 (2021).
2. Tschoegl, N. W. *The phenomenological theory of linear viscoelastic behavior: an introduction*; (Springer-Verlag Berlin Heidelberg, Berlin/Heidelbere, 1989).
3. Gautier A, Carpentier B, Dufresne M, Vu Dinh Q, Paullier P, Legallais C. Impact of alginate type and bead diameter on mass transfers and the metabolic activities of encapsulated C3A cells in bioartificial liver applications. *Eur. Cell Mater.* **21**, 94-106 (2011).
4. Pamies R, Schmidt RR, Martínez MdCL, Torre JGJCP. The influence of mono and divalent cations on dilute and non-dilute aqueous solutions of sodium alginates. *Carbohydr. Polym*. **80**, 248-253 (2010)
5. Topuz F, Henke A, Richtering W, Groll J. Magnesium ions and alginate do form hydrogels: a rheological study. *Soft Matter.* **8**, 4877-4881 (2012)
6. Plimpton S. Fast Parallel Algorithms for Short-Range Molecular Dynamics. *J. Comp. Phys.* **117**, 1-19 (1995).